ChemComm

ROYAL SOCIETY OF CHEMISTRY

FEATURE ARTICLE

Check for updates

Cite this: *Chem. Commun.*, 2021, **57**, 11301

Long-lived localised singlet diradicaloids with carbon–carbon π-single bonding (C–π–C)

Zhe Wang, Pinky Yadav and Manabu Abe *

Received 18th August 2021,
Accepted 27th September 2021

DOI: 10.1039/d1cc04581d

rsc.li/chemcomm

Localised singlet cyclopentane-1,3-diyl diradicaloids have been considered promising candidates for constructing carbon–carbon π-single bonds (C–π–C). However, the high reactivity during formation of the σ-bond has limited a deeper investigation of its unique chemical properties. In this feature article, recent progress in kinetic stabilisation based on the "stretch effect" and the "solvent dynamic effect" induced by the macrocyclic system is summarised. Singlet diradicaloids S-**DR4a/b** and S-**DR4d** containing macrocyclic rings showed much longer lifetimes at 293 K (14 μs for S-**DR4a** and 156 μs for S-**DR4b** in benzene) compared to the parent singlet diradicaloid S-**DR2** having no macrocyclic ring (209 ns in benzene). Furthermore, the dynamic solvent effect in viscous solvents was observed for the first time in intramolecular σ-bond formation, the lifetime of S-**DR4d** increased to 400 μs in the viscous solvent glycerin triacetin at 293 K. The experimental results proved the validity of the "stretch effect" and the "solvent dynamic effect" on the kinetic stabilisation of singlet cyclopentane-1,3-diyl diradicaloids, and provided a strategy for isolating the carbon–carbon π-single bonded species (C–π–C), and towards a deeper understanding of the nature of chemical bonding.

Introduction

The molecular structures and reactivities of compounds are largely dependent on their bonding styles and electronic structures, respectively. In this context, both the σ- and π-bonds are well-known fundamental bonds in carbon–carbon bonding systems (Fig. 1a), wherein σ-bonds are energetically stronger than π-bonds. As a result, π-electronic systems play important roles in various molecular functions, such as light absorption and redox processes. As in ethylene, π-bonding is generally possible with a strong σ-bond framework. Molecules containing π-single bond (C–π–C) systems, in which carbon atoms are not connected by σ-bonding, are expected to show unique molecular properties due to small HOMO–LUMO energy gaps and planar four-coordinated carbon atoms (Fig. 1a).[1–7]

Department of Chemistry, Graduate School of Advanced Science and Engineering, Hiroshima University, 1-3-1 Kagamiyama, Higashi-Hiroshima, Hiroshima 739-8526, Japan. E-mail: mabe@hiroshima-u.ac.jp

Zhe Wang

Zhe Wang was born in Qingdao, P. R. China. He received his bachelor's degree (BEng) from the China University of Petroleum (East China) in 2017. He then joined the research group of Professor Dr Abe at Hiroshima University. He received his master's degree (MSc) from the Hiroshima University in 2019 under the supervision of Professor Dr Manabu Abe. He is currently a PhD student at Hiroshima University. His research focuses on the kinetic stabilisation of singlet 2,2-dimethoxycyclopentane-1,3-diyl diradicals.

Pinky Yadav

Pinky Yadav received her PhD in chemistry from the Indian Institute of Technology, Roorkee, India in 2017 under the guidance of Prof. M. Sankar. After a post-doctoral stint at the Technion-Israel Institute of Technology, Haifa, Israel under the supervision of Prof. Z. Gross (2017–2020), she moved to Hiroshima University to work with Prof. M. Abe as an Assistant Professor (specially appointed) in 2021. Her research interest focuses on the study of cyclopentane-1,3-diyl and porphyrinoid diradical systems.

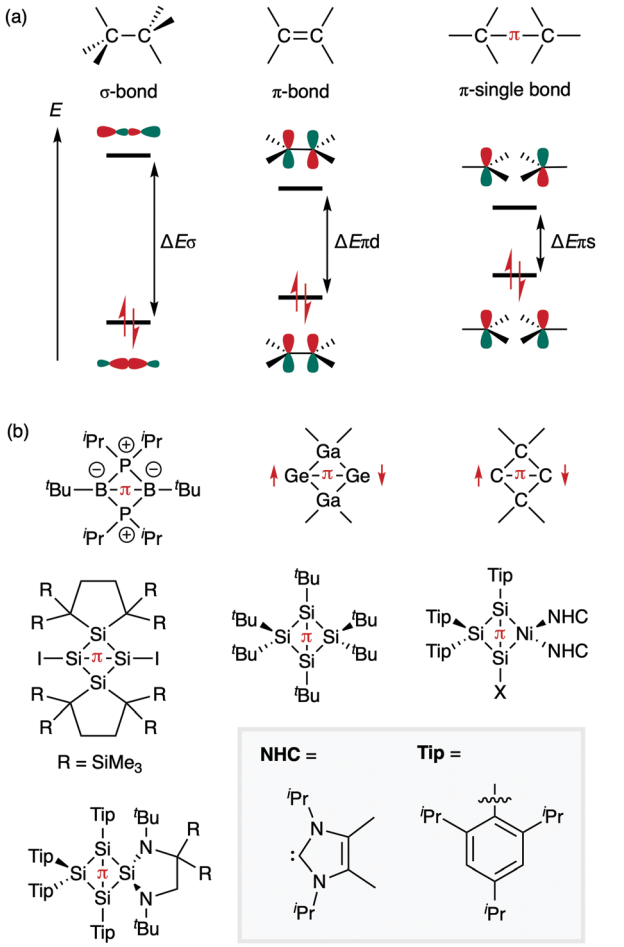

Fig. 1 (a) Bond styles in carbon–carbon connections; (b) reported singlet diradicaloids with B–B, Ge–Ge, C–C and Si–Si π single bonding.

In the period 1998–2000, our research group, in collaboration with Adam and Borden, reported that the ground state of

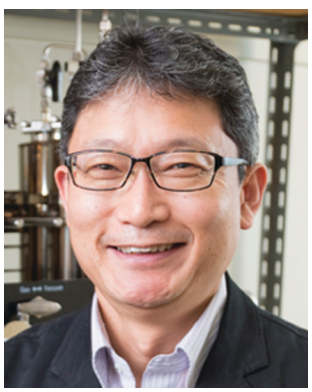

Manabu Abe

Manabu Abe was born in Osaka, Japan. He received his PhD from the Kyoto Institute of Technology with Professor Akira Oku, in 1995. In 1995, he became faculty staff at Osaka University (Prof. Masatomo Nojima's group). From 1997–1998, he was an Alexander-von-Humboldt fellow with Professor Dr Waldemar Adam at the Universität Würzburg. He was also a visiting researcher at the LMU München (Professor Dr Herbert Mayr) in 2007. He moved to Hiroshima and became a full-time professor of Organic Chemistry at the Department of Chemistry, Hiroshima University in 2007. His research focuses on reactive intermediate chemistry, especially diradicals.

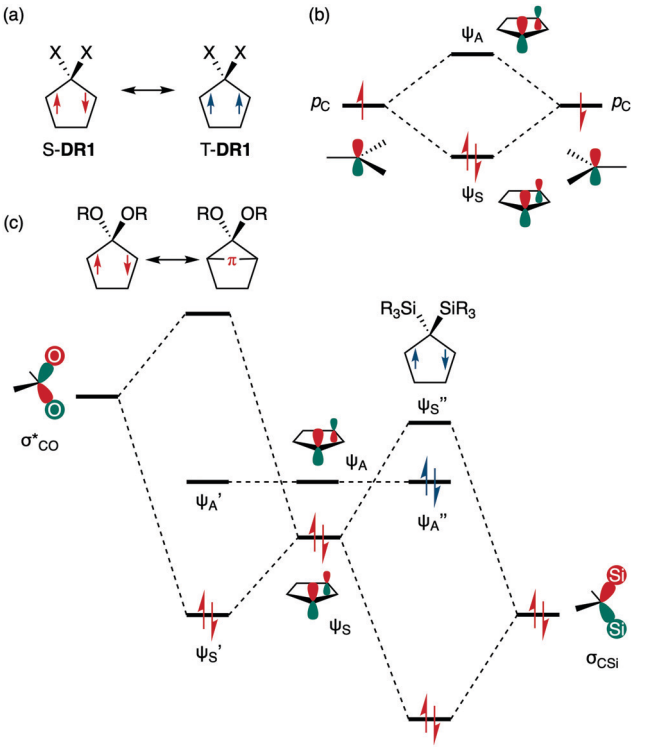

Fig. 2 (a) Singlet diradicaloids, possible candidates for carbon–carbon π single bonds; (b) through-space interaction between the 2p orbitals; (c) through-bond interaction between the σ/σ* and ψ_S orbitals.

cyclopentane-1,3-diyl diradicals **DR1** and their most stable electronic configurations (*i.e.*, the singlet and triplet state of spin multiplicity, indicated by the prefix "S-" and "T-") can be controlled by the substituent X effect at the C2 carbon atom (Fig. 2a).[8–10] In the case of cyclopentane-1,3-diyl species the singlet state has, in principle, a chance to possess the π-single bond (C–π–C).

The most stable ground state electronic configuration of the diradicaloids can be determined by through-space and through-bond interactions.[11–16] As shown in Fig. 2b, the through-space interaction between the two p orbitals at the C1 and C3 positions produces two molecular orbitals, namely the bonding orbital ψ_S and the antibonding orbital ψ_A. The through-bond interaction between the resulting bonding orbital ψ_S and the pseudo-π orbitals σ/σ* of the C2 substituent determine the ground state spin multiplicity and the most stable electronic configuration. Thus, the low-lying σ* (in Fig. 2, X = an electron-withdrawing group, such as F or OR) can stabilise ψ_S to increase the energy spacing between ψ_S' and ψ_A', ultimately leading to the singlet ground state of **DR1** with π-single bonding. On the other hand, the interaction with the high-lying σ (X = an electron-donating group such as H, CH_3, or SiR_3) destabilises ψ_S, which results in ψ_S'' being higher in energy than ψ_A'' (Fig. 2c).[17] In this case, singlet diradical species does not show π-single bonding between the radical–radical carbon centres. Thus, electron-withdrawing C2-substituents play a crucial role in the formation of π-single bonds in

 This journal is © The Royal Society of Chemistry 2021

cyclopentane-1,3-diyl diradicals. Recently, singlet diradicaloids exhibiting B–B, Ge–Ge, and Si–Si π-single bonding have been experimental examined by Bertrand,[18] Frenking,[19] Iwamoto,[20] Kyushin,[21] and Scheschkewitz,[22] and cyclobutane-1,3-diyls with C–C π-single bonding have been computationally predicted by Abe[23] (Fig. 1b).

The thermodynamic stabilisation of the highly reactive singlet cyclopentane-1,3-diyl diradical S-**DR1** has been achieved by introducing aryl groups at the 1,3-positions to extend the spin-delocalisation.[10] However, the thermodynamic stabilisation decreases the π-single bonding. The kinetic stabilisation of reactive species is a useful method for increasing the energy barrier of their chemical reactions to prolong their lifetimes (Fig. 3a).[24,25] Previously, we have succeeded in the kinetic stabilisation of singlet diradicaloids exhibiting π-single bonding through the steric hindrance originating from the steric repulsion between the bulky aryl groups (Ar) at the C1 and C3 position, and the alkoxy groups (OR) at the C2 position (Fig. 3bi).[26,27] For example, the lifetime of S-**DR3d** (singlet diradical **3d**, R_1 = Tip) was found to be 23.8 μs at 293 K, which is approximately 45 times longer than that of the parent S-**DR3a** (Fig. 4).[27]

In 2012, a new concept of the "stretch effect" was computationally proposed by our research group for the kinetic stabilisation of singlet diradicaloids (S-**DR**) embedded in macrocyclic structures.[28] The strain energies induced by the macrocyclic skeletons are proposed to increase during the σ-bond formation process. The σ-bond is expected to be stretched by the macrocyclic structure (Fig. 3bii). The increased molecular strain in the σ-bonded product (**CP**) energetically destabilises the transition states (**TS**) for the σ-bond formation. Thus, the singlet diradicaloids can be kinetically stabilised to increase their lifetimes. Experimental proof of the stretch effect was first reported in 2018 for S-**DR4a** and its dioctyl-substituted derivative S-**DR4b** with lifetimes of 14.0 and 14.2 μs, respectively at 293 K in benzene (Fig. 4).[29] In 2021, S-**DR4d** in a smaller macrocycle with a naphthyl moiety was reported for the first time with a significantly longer lifetime (τ_{293} = 155.9 μs in benzene at 293 K, Fig. 4) and the dynamic solvent effect in the σ-bond formation processes.[30] In this feature article, our focus will be on recent studies of the influence of the stretch effect and the solvent dynamic effect on kinetic stabilisation of localised singlet diradicaloids with π-single bond.

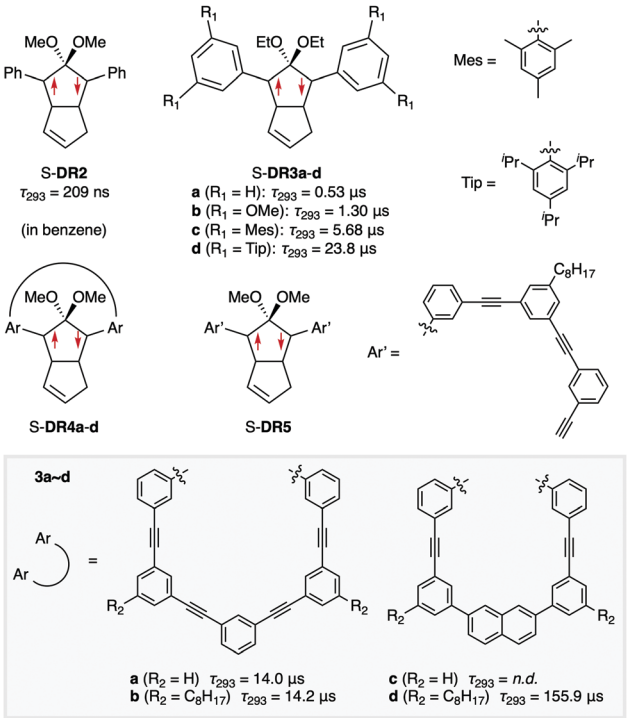

Fig. 4 Chemical structures of singlet diradicals S-**DR** and their lifetimes in benzene at 293 K.

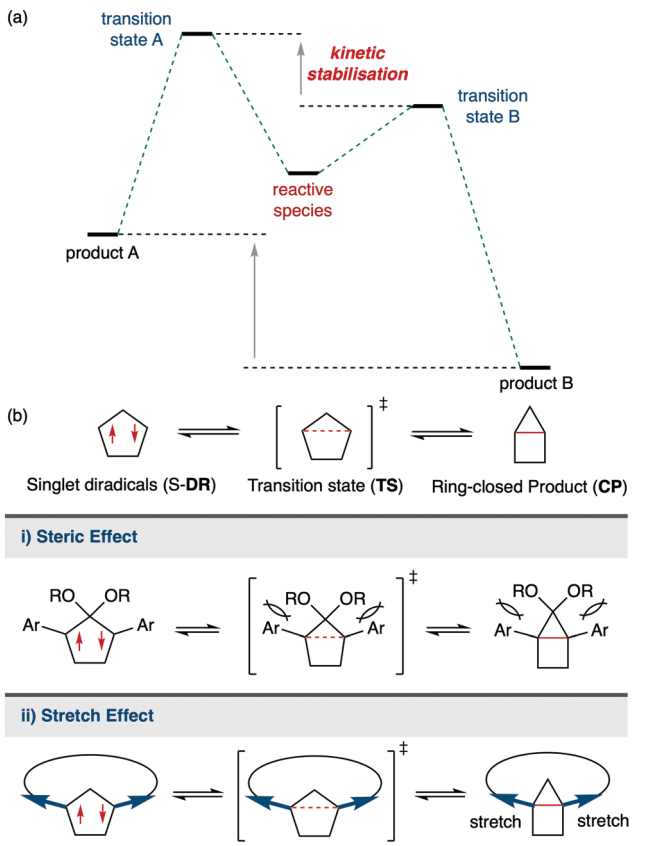

Fig. 3 (a) Schematic description of the kinetic stabilisation of a reactive species; (b) concept of the steric hinderance effect and stretch effect.

1. Molecular design of the stretch effect using quantum chemical calculations

The molecular design of the stretch effect should induce strain in σ-bonds that will lead to increases in the energy of the σ-bonded **CP** species.[29,30] To gain such an effect, macrocyclic skeletons with planar structures were designed as shown in S-**DR4a** and S-**DR4c**. According to the computational results, the formation of *cis*-configured σ-bonded products (*cis*-**CP**) was kinetically favoured over the thermodynamically favoured *trans*-configured σ-bonded products (*trans*-**CP**). The stretch effect in

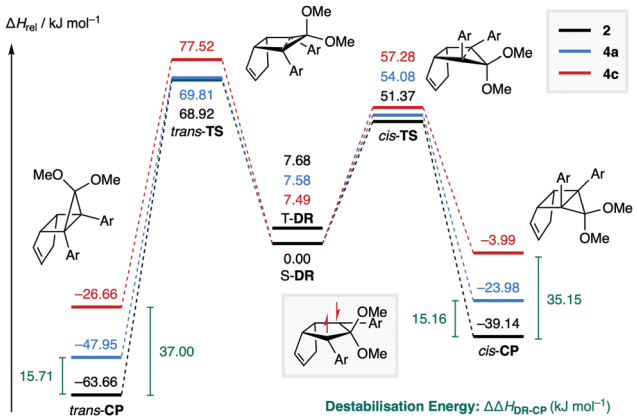

Fig. 5 Kinetic stabilisation on S-**DR4a** and S-**DR4c**. Calculated using the (R/U)ωB97X-D/6-31G(d) level of theory.

both molecules has been well proven by quantum chemical calculations using the (R/U)ωB97X-D/6-31G(d)[31–33] level of theory, which suggests that the σ-bonded products, *cis*-**CP4a/c** and *trans*-**CP4a/c**, were destabilised by energies ($\Delta\Delta H_{DR-CP}$) of 15.16/15.71 and 35.15/37.00 kJ mol^{-1}, respectively, compared to *cis*-/*trans*-**CP2** (Fig. 5 and Table 1). The increase of the molecular strain in the σ-bonded products was proven by computing the strain energies (SE) of macrocyclic species using isodesmotic reactions. As listed in Table 1, the destabilisation energies of the σ-bonded products **CP4** ($\Delta\Delta H_{DR-CP}$) were close to the strain energy relative to S-**DR4a** and S-**DR4c**, indicating that the increase of the energy of **CP4** is mainly derived from the strained structures induced by the macrocyclic skeletons. The molecular strain is the key factor in achieving the energetic destabilisation of σ-bonded products. In addition, the energy barriers for the σ-bonded compounds in S-**DR4** slightly increased compared to those in S-**DR2**, indicating destabilisation of the transition states **TS4**. These results suggest that S-**DR4a** and S-**DR4c** were kinetically stabilised by the stretch effect and were expected to be longer-lived than S-**DR2**.

The thermodynamic stabilisation derived from the macrocyclic structure in S-**DR4c** was compared with the parent S-**DR2** (Scheme 1). The reaction enthalpy (ΔH) was calculated to be 1.45 kJ mol^{-1} at the ωB97X-D/6-31G(d) level of theory, indicating that the macrocyclic skeleton with the meta-connection of the phenyl ring has a negligible influence on thermodynamic stabilisation of the singlet state in comparison with S-**DR2**. Thus, introduction of the macrocyclic skeleton kinetically stabilises the singlet diradicals.

Table 1 Strain energies calculated at the (R/U)ωB97X-D/6-31G(d) level of theory

Entry	Compound		SE	SE_{rel}	$\Delta\Delta H_{DR-CP}$
1	S-**DR4**	**a**	5.11	0.00	—
2		**c**	8.92	0.00	—
3	*cis*-**CP4**	**a**	19.63	14.52	15.16
4		**c**	43.66	34.74	35.15
5	*trans*-**CP4**	**a**	19.97	14.87	15.71
6		**c**	45.08	36.16	37.00

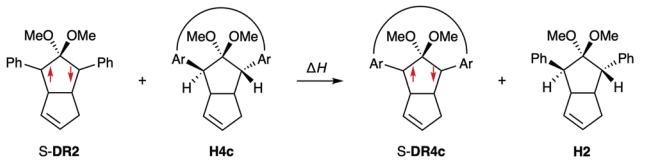

Scheme 1 Isodesmotic reaction for estimating thermodynamic stabilisation.

2. Stretch effect on the reactivity of singlet diradicaloids

Direct detection under low-temperature matrix conditions. First, the singlet diradicaloids S-**DR4a/d** were generated and detected through low-temperature photolysis of the corresponding azoalkanes **AZ4a/d** (Fig. 6, top) under matrix conditions.[29,30] During the photolysis of **AZ4a** and **AZ4d**, low-temperature UV-vis absorption spectra were recorded in a degassed 2-methyltetrahydrofuran (MTHF) glassy matrix at 90 K under irradiation with a xenon lamp (λ_{exc} = 360 ± 10 nm), respectively (Fig. 6). During irradiation of both **AZ4a** (Fig. 6a) and **AZ4d** (Fig. 6b), two absorption bands were observed at approximately 470 and 580 nm. After irradiation, the absorption band at 470 nm was diminished within seconds, whereas the 580 nm band persisted for several hours at 90 K, indicating that the absorption band at 470 and 580 nm could be assigned to the electronically excited states and ground state intermediates, respectively. The visible band at 580 nm corresponds to the π–π* electronic transition of the π-single bond (C–π–C).[34]

To clarify the transient species observed at ∼470 nm, low temperature electron-paramagnetic resonance (EPR) spectroscopy was conducted at 80 K in an MTHF glassy matrix (Fig. 7). During the photolysis of **AZ4a** and **AZ4d**, typical triplet EPR signals were observed. For **AZ4a** (Fig. 7a), the signals were observed at 2049 (z_1), 2682 (x_1, y_1), 3944 (x_2, y_2) and 4676 (z_2) G for the allowed transition ($|m_s|$ = 1), with a half-field signal ($|m_s|$ = 2) at 1512 G. The D/hc and E/hc were determined to be 0.12 and <0.001 cm^{-1}, respectively. The D value was much larger than a typical triplet 1,3-diphenyl cyclopentane-1,3-diyl diradical, which is known to be about 0.05 cm^{-1}, but quite similar to those of the triplet state of benzene derivatives (0.12–0.15 cm^{-1}). For **AZ4d** (Fig. 7b), similar triplet EPR signals were observed at 1571 (half-field), 2331 (z_1), 2507 (y_1), 3097 (x_1), 3509 (x_2), 4154 (y_2) and 4375 (z_2) G, with D/hc = 0.096 cm^{-1} and E/hc = 0.019 cm^{-1}. The zero-field splitting (zfs) parameters are quite close to those of the triplet excited state of 2-phenylnaphthalene (D/hc = 0.0963 cm^{-1} and E/hc = 0.0274 cm^{-1}). After the irradiation, the triplet EPR signals disappeared in seconds. The lifetime of the EPR active species was 2.5 s, indicating that the ∼470 nm species is assigned to the triplet excited state of the aromatic moiety in the macrocyclic ring, rather than triplet cyclopentane-1,3-diyl diradicals T-**DR4a/d**.

Direct detection and reaction dynamics of singlet diradicaloids at room temperature. The laser flash photolysis of azoalkanes **AZ4a/d** (Fig. 8, top) was conducted to allow the direct detection of S-**DR4a/d** and to analyse the reaction dynamics using transient absorption (TA) spectroscopy in benzene at

 This journal is © The Royal Society of Chemistry 2021

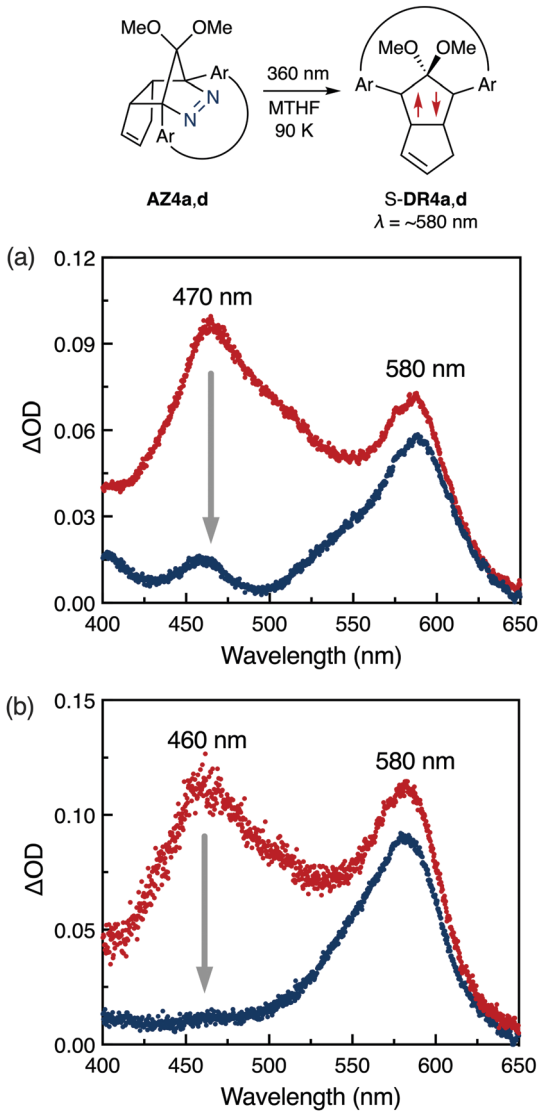

Fig. 6 UV-vis absorption spectroscopic analysis of the photolysis of (a) **AZ4a** and (b) **AZ4d** with a Xenon lamp in an MTHF matrix at 90 K. Red line: during irradiation; blue line: under dark conditions for 3/6 minutes after irradiation of **AZ4a/d**.

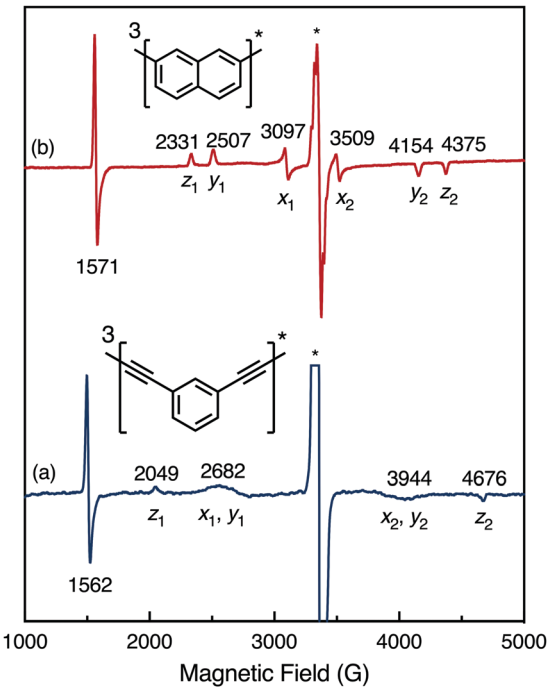

Fig. 7 EPR spectra during the photolysis of (a) **AZ4a** and (b) **AZ4d**.

293 K (Fig. 8, Table 2).[29,30] During the flash photolysis of **AZ4a** and **AZ4d**, two transient species were observed at approximately 470 and 580 nm under a nitrogen atmosphere (Fig. 8a and b). It was found that these species show absorptions at ~470 nm, which were quenched by oxygen under air, while the species exhibiting 580 nm bands show identical decay rate constants under both nitrogen and air. In addition, the 470 nm species have similar lifetimes during the photolysis of **AZ4a** (τ_{293} = 2.1 μs, Fig. 8c) and **AZ4d** (τ_{293} = 3.1 μs, Fig. 8d) under a nitrogen atmosphere, indicating that this transient species is derived from the triplet excited state of the aromatic ring in the macrocyclic skeleton, as found in Fig. 7.[29] The absorption band located at the 500–600 nm region was assigned to the π–π* electronic transition of the π-single bond (C–π–C) of S-**DR4**. The lifetime of S-**DR4a** was found to be 14.0 μs in benzene at 293 K (Fig. 8e, entry 2 in Table 2), which was approximately 70 times longer compared to the non-cyclic S-**DR2** (τ_{293} = 209 ns).[35] A similar TA was also observed for S-**DR4b** bearing an alkyl chain (Table 2, entry 3). Furthermore, the lifetime of S-**DR4b** was determined to be 14.2 μs in benzene at 293 K, which was nearly identical to S-**DR4a** (entry 2), while the singlet diradicaloid S-**DR4d** exhibited a much longer lifetime of 155.9 μs under the same experimental conditions (Fig. 8f, entry 4 in Table 2),[30] thereby it is demonstrated that the kinetic stabilisation induced by the macrocyclic ring plays a crucial role in increasing the lifetime.

Variable temperature TA (VT-TA) measurements were conducted to determine the activation parameters of the σ-bond formation process (*i.e.*, E_a, log$A$, $\Delta H^{\ddagger}$, $\Delta S^{\ddagger}$, and $\Delta G^{\ddagger}_{293}$, Table 2).[29,30] As predicted by computational calculations, the activation energies and enthalpies of the ring-closing processes of S-**DR4a**, S-**DR4b**, and S-**DR4d** were increased by approximately 20, 20, and 30 kJ mol^{-1}, respectively, compared to the corresponding values of S-**DR2**, and this was attributed to kinetic stabilisation of the singlet diradicals by the macrocyclic ring effect (Table 2, entries 1–4). In addition, the large log$A$ value (>12) suggests that the spin-allowed decay of the singlet diradicaloids took place. Although the activation entropies showed positive values for the various S-**DR4** species, a negative value was found for the decay process of S-**DR2**.

TA analysis of **AZ5** in Fig. 4, which is a byproduct of the synthesis of **AZ4b**, was conducted to understand the macrocyclic effect. As expected, the lifetime of S-**DR5** was 620 ns, which is significantly shorter than that of S-**DR4b** (entry 5 in Table 2).[29] The VT-TA experiments also revealed that the activation parameters of the decay process of S-**DR5** were

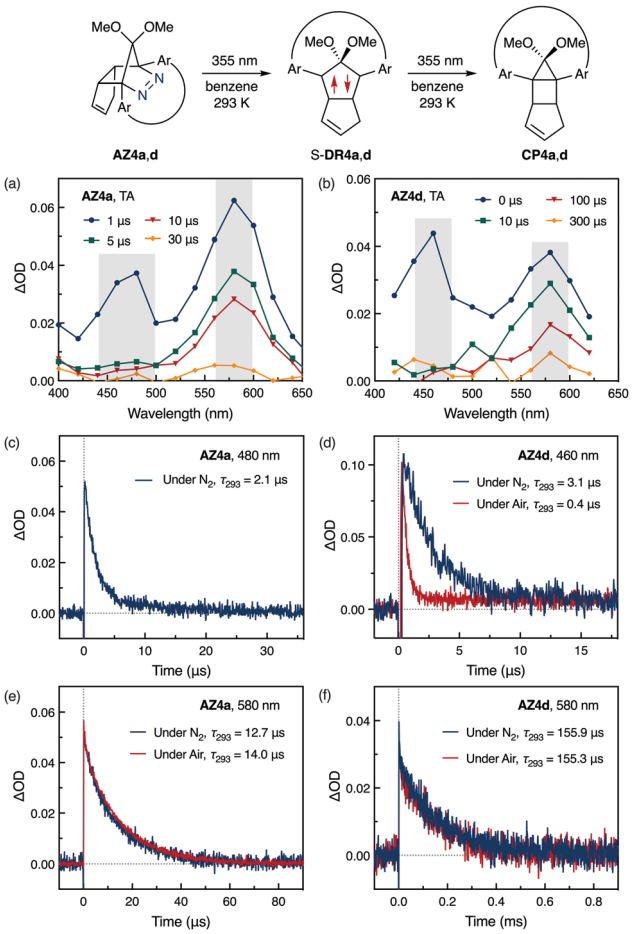

Fig. 8 Transient absorption (TA) spectra observed in the laser flash photolysis of (a) **AZ4a** and (b) **AZ4d** under a nitrogen atmosphere. Time profiles for the photolysis of **AZ4a** at (c) 480 and (e) 580 nm, and **AZ4d** at (d) 460 and (f) 580 nm.

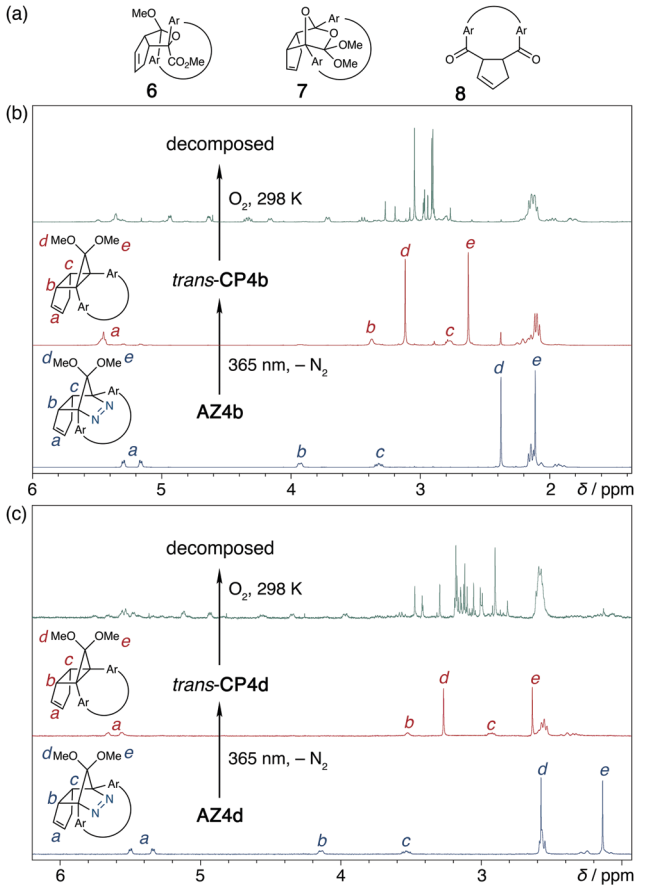

Fig. 9 (a) Chemical structures of oxidized products **6**, **7** and **8**. *In situ* ^{1}H NMR (400 MHz) analysis of the photoreaction of (b) **AZ4b** and (c) **AZ4d**.

similar to those of S-**DR2**. Thus, the stretch effect induced by the macrocyclic structure is the key factor in enhancing the lifetimes of singlet diradicaloids.

3. Influence of the stretch effect on the reactivity of CP4

To investigate the influence of the stretch effect on the reactivity of **CP4b/d**, benzene-d_6 solutions of azoalkanes **AZ4b** and **AZ4d** were degassed and sealed under a nitrogen atmosphere in NMR tubes, and the photoreactions were directly monitored using ^{1}H NMR spectroscopy (Fig. 9). The clean denitrogenation ($\Phi > 0.9$) of azoalkanes **AZ4b** and **AZ4d** quantitatively yielded the σ-bonded compounds *trans*-**CP4b** and *trans*-**CP4d**. The stereochemistry of the products was determined using Nuclear Overhauser effect measurements (NOE). Formation of the thermodynamically stable *trans*-**CP2** was confirmed in the photolysis of **AZ2**, although a higher energy barrier was computed for the formation of the *trans* isomers compared to the *cis* isomers (Fig. 5). This contradiction was solved by conducting low-temperature NMR analysis, which shows the selective formation of the *cis* isomers was observed in the photolysis ($h\nu = 355$ nm) while their isomerisation to the *trans* isomers was detected under thermal conditions (*vide infra* in Fig. 10).

The σ-bonded compounds *trans*-**CP4b** and *trans*-**CP4d** show high reactivity towards oxygen at room temperature (*i.e.*, 298 K) which results in the formation of oxygenated products **6–8**. However, *trans*-**CP2** was not decomposed under the same reaction conditions, but it was observed upon heating up to

Table 2 Lifetimes of the singlet diradicals S-**DR** at 293 K and the activation parameters (E_a, log A, $\Delta H^{\ddagger}$, $\Delta S^{\ddagger}$, and $\Delta G^{\ddagger}_{293}$) of the ring-closing process in benzene

Entry	S-**DR**	τ_{293}/μs	E_a/kJ mol^{-1}	log A/s^{-1}	$\Delta H^{\ddagger}$/kJ mol^{-1}	$\Delta S^{\ddagger}$/J mol^{-1} K^{-1}	$\Delta G^{\ddagger}_{293}$/kJ mol^{-1}
1	**2**	0.21 ± 0.01	30.5 ± 0.4	12.1 ± 0.1	28.0 ± 0.4	−21.5 ± 0.8	34.2 ± 0.8
2	**4a**	14.0 ± 1.1	55.4 ± 0.7	14.7 ± 0.2	52.9 ± 0.7	28.4 ± 3.2	44.6 ± 0.9
3	**4b**	14.2 ± 0.8	52.3 ± 0.4	14.1 ± 0.1	49.7 ± 0.4	17.1 ± 1.2	44.7 ± 0.4
4	**4d**	155.9 ± 3.3	58.4 ± 1.1	14.2 ± 0.2	56.0 ± 1.1	18.1 ± 2.3	50.7 ± 1.1
5	**5**	0.62 ± 0.01	31.2 ± 0.8	11.7 ± 0.1	28.7 ± 0.8	−28.9 ± 2.7	37.2 ± 0.8

This journal is © The Royal Society of Chemistry 2021

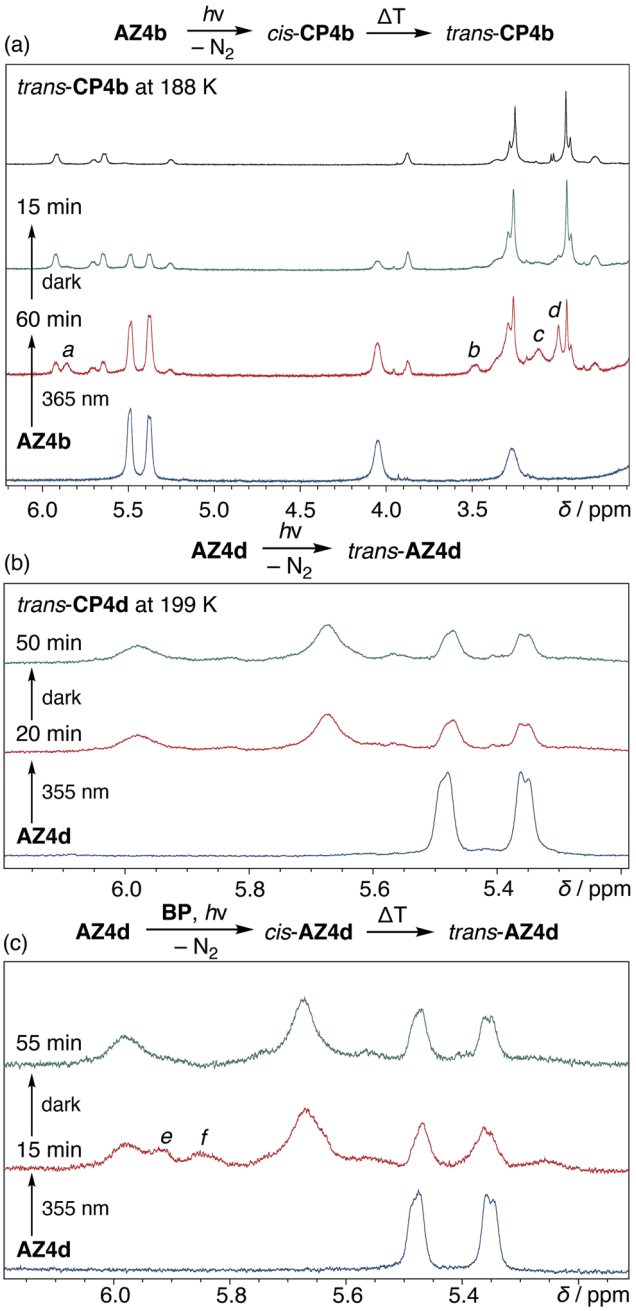

Fig. 10 *In situ* ^{1}H NMR (400 MHz) analysis of the photoreaction of (a) **AZ4b** and (b and c) **AZ4d** at low temperature.

353 K in air. The structures of the oxygenated products obtained from *trans*-**CP4a** and *trans*-**CP4b** were similar to those obtained from *trans*-**CP2**. All these products were derived from the endoperoxide intermediates (Scheme 2).[10]

4. Product analyses at low temperatures

According to the computational studies (Fig. 5), *cis*-**CP4b/d** should be the major photoproduct in the photochemical denitrogenation of **AZ4b/d**, as smaller energy barriers were computed for the *cis* isomer compared to those of the *trans* isomer. However, the exclusive formation of *trans*-**CP4b** and *trans*-**CP4d** at 298 K suggests that fast

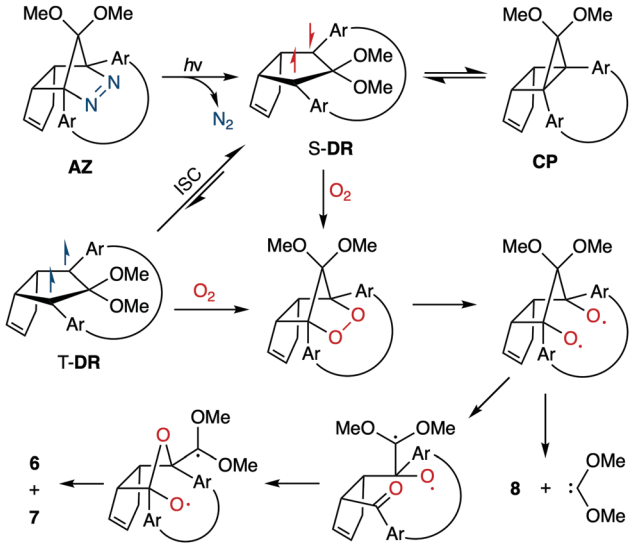

Scheme 2 Proposed oxidation reaction mechanism for the decomposition of σ-bonded products.

isomerisation took place from *cis*-**CP4b/d** to *trans*-**CP4b/d** *via* S-**DR4b/d**. This isomerisation should be suppressed at low temperatures owing to the relatively large energy barrier between S-**DR4b/d** and *trans*-**CP4b/d**. To observe the kinetically favoured compound *cis*-**CP4b/d**, low-temperature *in situ* ^{1}H NMR analyses of the photolysis of **AZ4b** and **AZ4d** were conducted in a degassed toluene-d_8 solution in sealed NMR tubes (Fig. 10).

Interestingly, during the photolysis of **AZ4b** thermally labile species (signals a–d) were observed along with *trans*-**CP4b** and unreacted **AZ4b** at 188 K using a 355 nm Nd:YAG laser. Signals a–d started to disappear with a concomitant increase in the signals corresponding to *trans*-**CP4b** after a 15 min reaction in dark conditions (Fig. 10a). The photolysis reaction of **AZ4d** does not produce any new signals under direct irradiation at 199 K except those originating from *trans*-**CP4d** (Fig. 10b). New signals (e–f) were observed during the irradiation of **AZ4d** at 199 K in the presence of the triplet sensitizer, benzophenone, which further converted into *trans*-**CP4d** under dark conditions over 55 minutes (Fig. 10c). According to the activation energies determined using the VT-LFP experiments (Table 2), the lifetime of S-**DR4b** at 188 K is approximately 1 second while the lifetime of S-**DR4d** at 199 K is close to 13 seconds. The new signals observed during the low-temperature photolysis of **AZ4b** and **AZ4d** are relatively long-lived over approximately 6 minutes and possibly correspond to *cis*-**CP4b** and *cis*-**CP4d**, rather than S-**DR4b** and S-**DR4d**. Interestingly, after irradiation, the formation of *trans*-**CP4d** at 199 K without a triplet sensitizer could be explained by the existence of the puckered-type diradical *puc*-S-**DR4d** (Path A in Scheme 3), while the benzophenone-sensitisation gives *cis*-**CP4d**, which involved the formation of a more stable planar *pl*-S-**DR4d** (Path B in Scheme 3).

5. Solvent dynamic effect[36] on the reactivity of singlet diradicaloids exhibiting the stretch effect

The influence of the solvent effect on the reactivities of singlet cyclopentane-1,3-diyl diradicaloids was examined in 13 solvents

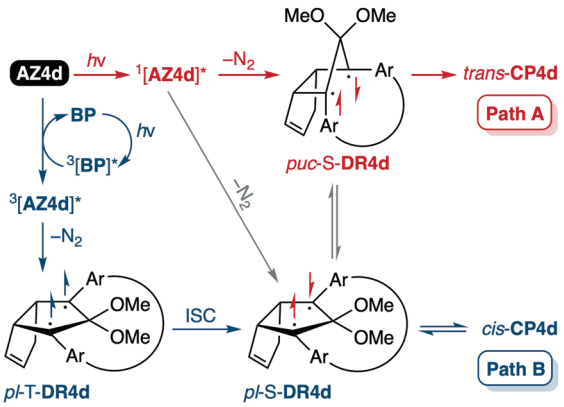

Scheme 3 Possible decay pathways for the photoexcitation reactions of **AZ4b** and **AZ4d**.

with a wide range of polarity (π^*)[37,38] and viscosity (η)[39] (Table 3). As depicted from the table data (the order of solvent polarity and lifetime of S-**DR2** is indicated by the number in parentheses), the lifetime of S-**DR2** largely depends on the solvent polarity, a longer lifetime was observed at higher solvent polarities, which suggests that S-**DR2** possesses a zwitterionic character (Scheme 4).[10] Interestingly, the influence of viscosity of the solvent also affects the lifetime of S-**DR2** and S-**DR4d**. For instance, the singlet diradicaloid S-**DR4d** was found to be extremely long-lived (400.2 μs) in glycerine triacetate (η = 23.00 cP, π^* = 0.63 kcal mol^{-1}), which was more than 14 times longer than that recorded in acetone (η = 0.32 cP, π^* = 0.62 kcal mol^{-1}, τ_{293} = 27.9 μs), although the polarity of acetone and glycerine triacetate are relatively similar (entries 8 and 9). In the case of S-**DR2**, the effect of solvent viscosity on the lifetime was much smaller than that observed in S-**DR4d** (entries 8 and 9).

The correlation between the rate constant k (= $1/\tau_{293}$) of the radical–radical coupling reaction, and solvent polarity/viscosity are shown in Fig. 11. For the non-cyclic diradical S-**DR2**, a good relationship between log k and solvent polarity (Fig. 11a) was observed, although the data point obtained in glycerin triacetate was deviated from the linear correlation due to its high

Table 3 Lifetimes τ_{293} of S-**DR2** and S-**DR4d** at 293 K in different solvents with varying polarity (π^*) and viscosity (η) properties

Entry	Solvent	π^*/kcal mol^{-1}	η (20 °C)/cP	τ_{293} of S-**DR2**/ns	τ_{293} of S-**DR4d**/μs
1	*n*-Hexane	−0.11 (1)	0.31 (2)	90.1 (1)	N.D.
2	Carbon tetrachloride	0.21 (2)	0.97 (10)	187.1 (5)	17.2 (1)
3	Diethyl ether	0.24 (3)	0.24 (1)	136.3 (2)	46.8 (5)
4	Ethyl acetate	0.45 (4)	0.46 (5)	182.6 (4)	73.1 (8)
5	Toluene	0.49 (5)	0.59 (7)	170.4 (3)	116.5 (10)
6	1,4-Dioxane	0.49 (5)	1.18 (11)	250.6 (8)	61.4 (6)
7	Benzene	0.55 (7)	0.65 (8)	210.0 (6)	155.9 (11)
8	Acetone	0.62 (8)	0.32 (3)	231.4 (7)	27.9 (3)
9	Glycerin triacetate	0.63 (9)	23.00 (13)	517.1 (13)	400.2 (12)
10	Chloroform	0.69 (10)	0.58 (6)	404.8 (12)	65.4 (7)
11	Dichloromethane	0.73 (11)	0.44 (4)	294.0 (9)	46.6 (4)
12	1,2-Dichloroethane	0.73 (11)	0.79 (9)	307.6 (10)	22.8 (2)
13	Dimethyl sulfoxide	1.00 (13)	2.24 (12)	393.5 (11)	95.1 (9)

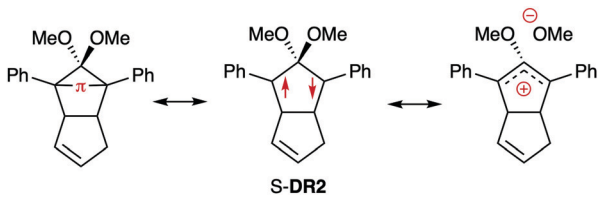

Scheme 4 Resonance structures in the singlet diradical S-**DR2**.

viscosity. For S-**DR4d**, the good correlation was not observed for either solvent polarity or viscosity alone (Fig. 11c and d). Thus, both the viscosity and polarity of the solvent should be considered in the solvent effect on the reactivity of singlet diradicals.

The contributions of solvent polarity and viscosity on the diradical lifetimes were analysed by regression analysis using eqn (1) with all data points shown in Table 3, which contains the polarity term $A\pi^*$, the viscosity term $B\eta$ and a constant C (Table 4). In the case of S-**DR2**, the polarity of the solvent was the dominant factor in determining the lifetime where coefficient A is much larger than coefficient B. In contrast to S-**DR2**, coefficients A and B were of the same magnitude for S-**DR4d** suggesting that the solvent polarity and viscosity both have a significant influence on the lifetime of S-**DR4d**. A good linear correlation between the experimental lifetime values and the predicted lifetime determined using eqn (1) was observed, despite the fact that the data points corresponding to benzene and toluene in S-**DR4d** and chloroform in S-**DR2** deviated slightly from the fitting line (Fig. 12).

Summary and outlook

Approximately a decade has passed since the concept of the "stretch effect" emerged. Our research group has reported two studies on S-**DR4a/b** and S-**DR4d** based on experimental results

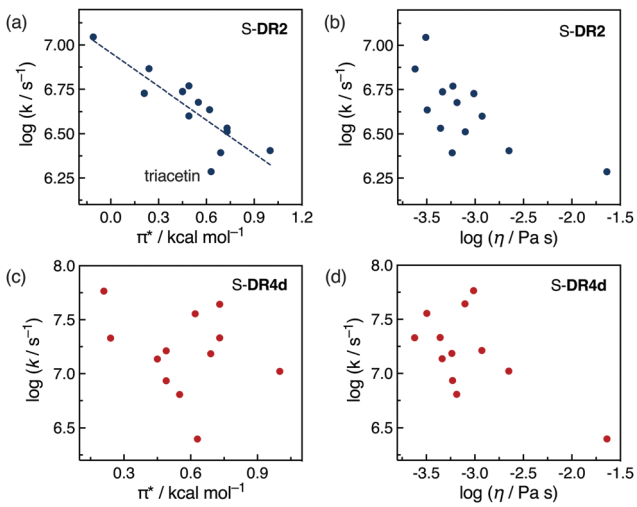

Fig. 11 Correlations between the radical–radical coupling rate constant log k and the solvent polarity (π^*) and viscosity (η) for (a and b) S-**DR2** and (c and d) S-**DR4d**.

 This journal is © The Royal Society of Chemistry 2021

Table 4 Regression analyses for the lifetimes and solvent parameters of S-**DR2** and S-**DR4d**

$\tau = A\pi^* + B\eta + C$ (1)

Coefficient	*A*	*B*	*C*
S-**DR2**	278.43	11.06	88.69
S-**DR4d**	15985.07	14940.91	45794.25

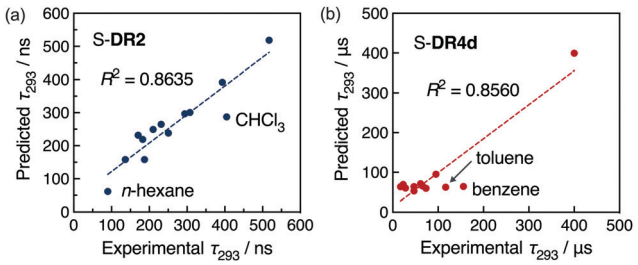

Fig. 12 Correlation diagram between the experimental and theoretically calculated lifetime for (a) S-**DR2** and (b) S-**DR4d**.

of the kinetic stabilisation of localised singlet diradicals using the stretch effect. S-**DR4a** and S-**DR4b** showed an approximate lifetime of 14 μs, whereas the lifetime of S-**DR4d,** which was constructed with a smaller macrocyclic ring, was found to be 1000 times longer (*i.e.*, 156 μs at 293 K in benzene) compared to the non-macrocyclic S-**DR2**. Further, the σ-bonded compound *trans*-**CP4** was found to be thermally labile under aerobic conditions due to the molecular strain derived from the macrocyclic skeleton, which resulted in rapid decomposition *via* an endoperoxide intermediate. However, the non-macrocyclic *trans*-**CP2** was stable under air even at 353 K. As predicted by theoretical calculations, isomerisation from *cis*-**CP4** to *trans*-**CP4** was observed at >199 K using *in situ* ^{1}H NMR analyses. According to the time-resolved laser flash photolysis measurements, the lifetime of non-macrocyclic S-**DR2** was mainly determined by the solvent polarity. However, in the case of S-**DR4d**, the solvent polarity and viscosity both played a crucial role in controlling the reactivity of S-**DR4d** in the solution phase. Currently, our research group is conducting further molecular designs and syntheses of singlet diradicaloids with π-single bonding for more detailed studies. The concept of kinetic stabilisation based on the "stretch effect"[28] and the "solvent dynamic effect"[36] will also be further applied to the kinetic stabilisation of other reactive species in future work.

Conflicts of interest

There are no conflicts to declare.

Acknowledgements

This work was supported by JSPS KAKENHI Grant Number 21H01921 (MA).

Notes and references

1 R. Hoffmann, R. W. Alder and C. F. Wilcox, *J. Am. Chem. Soc.*, 1970, **92**, 4992–4993.
2 J. B. Collins, J. D. Dill, E. D. Jemmis, Y. Apeloig, P. V. R. Schleyer, J. B. Collins, E. D. Jemmis, P. V. R. Schleyer, R. Seeger and J. A. Pople, *J. Am. Chem. Soc.*, 1976, **98**, 5419–5427.
3 U. Deva Priyakumar and G. Narahari Sastry, *Tetrahedron Lett.*, 2004, **45**, 1515–1517.
4 U. D. Priyakumar, A. S. Reddy and G. N. Sastry, *Tetrahedron Lett.*, 2004, **45**, 2495–2498.
5 B. Sateesh, A. Srinivas Reddy and G. Narahari Sastry, *J. Comput. Chem.*, 2007, **28**, 335–343.
6 O. J. Cooper, A. J. Wooles, J. McMaster, W. Lewis, A. J. Blake and S. T. Liddle, *Angew. Chem., Int. Ed.*, 2010, **49**, 5570–5573.
7 M. Abe and R. Akisaka, *Chem. Lett.*, 2017, **46**, 1586–1592.
8 M. Abe, W. Adam and W. M. Nau, *J. Am. Chem. Soc.*, 1998, **120**, 11304–11310.
9 W. Adam, W. T. Borden, C. Burda, H. Foster, T. Heidenfelder, M. Heubes, D. A. Hrovat, F. Kita, S. B. Lewis, D. Scheutzow and J. Wirz, *J. Am. Chem. Soc.*, 1998, **120**, 593–594.
10 M. Abe, W. Adam, T. Heidenfelder, W. M. Nau and X. Zhang, *J. Am. Chem. Soc.*, 2000, **122**, 2019–2026.
11 R. Hoffmann, *J. Am. Chem. Soc.*, 1968, **90**, 1475–1485.
12 R. Hoffmann, *Acc. Chem. Soc.*, 1971, **4**, 1–9.
13 L. Salem and C. Rowlaand, *Angew. Chem., Int. Ed. Engl.*, 1972, **11**, 92–111.
14 S. J. Getty, D. A. Hrovat and W. T. Borden, *J. Am. Chem. Soc.*, 1994, **116**, 1521–1527.
15 W. T. Borden, *Chem. Commun.*, 1998, 1919–1925.
16 (*a*) M. Abe, J. Ye and M. Mishima, *Chem. Soc. Rev.*, 2012, **41**, 3808–3820; (*b*) M. Abe, *Chem. Rev.*, 2013, **113**, 7011–7088.
17 M. Abe, S. Kawanami, C. Ishihara and M. Nojima, *J. Org. Chem.*, 2004, **69**, 5622–5626.
18 D. Scheschkewitz, H. Amii, H. Gornitzka, W. W. Schoeller, D. Bourissou and G. Bertrand, *Science*, 2002, **295**, 1880–1881.
19 A. Doddi, C. Gemel, M. Winter, R. A. Fischer, C. Goedecke, H. S. Rzepa and G. Frenking, *Angew. Chem., Int. Ed.*, 2013, **52**, 450–454.
20 T. Nukazawa and T. Iwamoto, *J. Am. Chem. Soc.*, 2020, **142**, 9920–9924.
21 S. Kyushin, Y. Kurosaki, K. Otsuka, H. Imai, S. Ishida, T. Kyomen, M. Hanaya and H. Matsumoto, *Nat. Commun.*, 2020, **11**, 4009.
22 (*a*) P. K. Majhi, M. Zimmer, B. Morgenstern and D. Scheschkewitz, *J. Am. Chem. Soc.*, 2021, **143**, 8981–8986; (*b*) C. B. Yildiz, K. I. Leszczyńska, S. González-Gallardo, M. Zimmer, A. Azizoglu, T. Biskup, C. W. M. Kay, V. Huch, H. S. Rzepa and D. Scheschkewitz, *Angew. Chem., Int. Ed.*, 2020, **59**, 15087–15092.
23 (*a*) Y. Fujita, M. Abe, Y. Shiota, T. Suzuki and K. Yoshizawa, *Bull. Chem. Soc. Jpn.*, 2016, **89**, 770–778; (*b*) M. Abe, C. Ishihara and M. Nojima, *J. Org. Chem.*, 2003, **68**, 1618–1621.
24 N. Tokitoh, T. Matsumoto and R. Okazaki, *Bull. Chem. Soc. Jpn.*, 1999, **72**, 1665–1684.
25 T. Matsuo and K. Tamao, *Bull. Chem. Soc. Jpn.*, 2015, **88**, 1201–1220.
26 J. Ye, Y. Fujiwara and M. Abe, *Beilstein J. Org. Chem.*, 2013, **9**, 925–933.
27 R. Akisaka and M. Abe, *Chem. – Asian J.*, 2019, **14**, 4223–4228.
28 M. Abe, H. Furunaga, D. Ma, L. Gagliardi and G. J. Bodwell, *J. Org. Chem.*, 2012, **77**, 7612–7619.
29 Y. Harada, Z. Wang, S. Kumashiro, S. Hatano and M. Abe, *Chem. – Eur. J.*, 2018, **24**, 14808–14815.
30 Z. Wang, R. Akisaka, S. Yabumoto, T. Nakagawa, S. Hatano and M. Abe, *Chem. Sci.*, 2021, **12**, 613–625.
31 J.-D. Chai and M. Head-Gordon, *Phys. Chem. Chem. Phys.*, 2008, **10**, 6615–6620.
32 W. J. Hehre, R. Ditchfield and J. A. Pople, *J. Chem. Phys.*, 1972, **56**, 2257–2261.
33 P. C. Hariharan and J. A. Pople, *Theor. Chim. Acta*, 1973, **28**, 213–222.
34 J. Ye, S. Hatano, M. Abe, R. Kishi, Y. Murata, M. Nakano and W. Adam, *Chem. – Eur. J.*, 2016, **22**, 2299–2306.
35 T. Nakagaki, T. Sakai, T. Mizuta, Y. Fujiwara and M. Abe, *Chem. – Eur. J.*, 2013, **19**, 10395–10404.
36 R. Akisaka, Y. Ohga and M. Abe, *Phys. Chem. Chem. Phys.*, 2020, **22**, 27949–27954.
37 M. J. Kamlet, J.-L. M. Abboud and R. W. Taft, *J. Am. Chem. Soc.*, 1977, **99**, 6027–6038.
38 C. Laurence, P. Nicolet, M. T. Dalati, J.-L. M. Abboud and R. Notario, *J. Phys. Chem.*, 1994, **98**, 5807–5816.
39 Physical Properties of Solvents, https://www.sigmaaldrich.com/content/dam/sigma-aldrich/docs/Aldrich/General_Informaion/labbasics_pg144.pdf.